



**HAL**  
open science

## Study of capillary interaction between two grains: a new experimental device with suction control

Jean-Philippe Gras, Jean-Yves Delenne, Moulay Saïd El Yousoufi

### ► To cite this version:

Jean-Philippe Gras, Jean-Yves Delenne, Moulay Saïd El Yousoufi. Study of capillary interaction between two grains: a new experimental device with suction control. *Granular Matter*, 2013, 15 (1), pp.49-56. 10.1007/s10035-012-0388-2 . hal-00844355

**HAL Id: hal-00844355**

**<https://hal.science/hal-00844355v1>**

Submitted on 20 Oct 2016

**HAL** is a multi-disciplinary open access archive for the deposit and dissemination of scientific research documents, whether they are published or not. The documents may come from teaching and research institutions in France or abroad, or from public or private research centers.

L'archive ouverte pluridisciplinaire **HAL**, est destinée au dépôt et à la diffusion de documents scientifiques de niveau recherche, publiés ou non, émanant des établissements d'enseignement et de recherche français ou étrangers, des laboratoires publics ou privés.

Copyright

# Study of capillary interaction between two grains: a new experimental device with suction control

J.-P. Gras · J.-Y. Delenne · M. S. El Youssoufi

**Abstract** We investigated the behavior of a water liquid bridge formed between two grains. We mainly focused on tensile tests with suction control (capillary pressure). Theo-retical and experimental studies are compared. A new exper-imental device involving suction control of the liquid bridge was developed specifically for this kind of test. Most of the liquid bridge variables and characteristics were measured by image analysis (gorge radius, volume, contact angles, fill-ing angles). Capillary force was measured by differential weighting. Experimental conditions allows us to avoid vis-cous effects. Our experimental results were close to Young-Laplace equation solutions. The “gorge method”, commonly used for calculating the capillary force, was also validated by our experiments. Liquid bridge rupture was studied and a new rupture criterion is proposed. This criterion depends on the grain radius, contact angle, surface tension and suction and was in agreement with the experimental results.

**Keywords** Capillarity · Liquid bridge · Tensile test · Suction · Experimental device · Rupture criterion

## 1 Introduction

Understanding the role of capillary interactions in the overall behaviour of a wet granular material is of considerable technological importance for applications in many fields, such as civil engineering, pharmaceutical research, agronomy, etc. Some properties, such as tensile strength and water reten-tion, strongly depend on the capillary interactions between grains. For example, sand castles may be sculpted when sand is mixed with water [1]. Liquid bridges between grains generate attractive forces when the water content is low enough. These forces are due to the surface tension  $\gamma$  and the difference between the air pressure  $p_a$  and the liquid pressure  $p_w$  across the liquid/air interface, also called suction. Know-ing the capillary force that generates such liquid bridges is important to determine the local origins of the mechanical behaviour of unsaturated granular media [2].

A stable liquid bridge can be obtained by controlling the suction or liquid volume. We decided to control the suc-tion in this study. One advantage is that the suction of every liquid bridge in a sample is equal to the macroscopic suction imposed upon a laboratory sample (at equilibrium). We put forth the hypothesis that the equilibrium of suction and liquid bridge volumes is achieved by the formation of a thin film of water at the grain surface, thus enabling a quite rapid return to equilibrium. For example, after mixing water with a gran-ular medium, the relaxation time of liquid bridge volumes is around 5 min [3].

Several theoretical studies on the behaviour of liquid bridges between two spherical grains have been carried out using numerical solution of the Young-Laplace equation or a method based on the approximation of liquid bridge pro-files via circles (toroidal approximation). In most cases, these studies involve tensile tests on liquid bridges with an imposed volume. Some expressions which link the capillary force, volume and geometrical and physical characteristics of the liquid bridge have been proposed for monodisperse [4,5] and polydisperse [6,7] cases. Recently, some authors have stud-ied the relation between suction and liquid bridge volume [8–11] for given interparticle distances. Monodisperse [8,9, 11] or polydisperse [10] grain-pairs were considered in these

J.-P. Gras (✉) · J.-Y. Delenne · M. S. El Youssoufi  
LMGC, CNRS, Université Montpellier 2, Montpellier, France  
e-mail: jean-philippe.gras@univ-montp2.fr

J.-Y. Delenne · M. S. El Youssoufi  
MIST Laboratory, IRSN, CNRS UMR 5508, Université Montpellier 2,  
Montpellier, France

studies. The toroidal approximation has been validated in monodisperse and polydisperse cases for given interparticle distances [8, 10]. Recently, tensile tests were briefly investigated with suction control [12], with a numerical resolution of the Laplace-Young equation.

Experiments have been carried out to study tensile tests on liquid bridges for a given volume. One of the first experimental studies was conducted by Mason and Clark [13], who measured the capillary force as a function of the interparticle distance between two monodisperse spheres or between a sphere and a plate. Since this experiment, several experimental studies have been carried out on polydisperse and monodisperse spheres [5, 14–17], with close agreement with Young-Laplace equation solutions. We should underline the experiments of Willet et al. [16] which seem very close to modelling results because of the use of spheres with an exceptional surface state. To our knowledge, however, no experimental studies have focused on liquid bridges with suction control.

In this paper, we present an original experimental device which allowed us to conduct tensile tests on liquid bridges with suction control. The results of this experiment are compared to Young-Laplace equation solutions, and the “gorge method” is tested to calculate the capillary force. Then, we present some results concerning the rupture distance.

## 2 Experimental setup

An experimental device was designed to perform displacement controlled tensile tests on capillary bridges between grain-pairs for a given suction (Fig. 1). A “grain-pair” is an assembly of two spherical grains linked by a liquid bridge. This device allows the measurement of capillary force as a function of displacement, suction control, and measurement of the main liquid bridge characteristics by image analysis.

### 2.1 Monitoring of tensile force as a function of displacement

The experimental device is shown in Figs. 1 and 2. A micrometer table associated with a computer-controlled step motor governs the vertical displacement of the upper bead fixed to the micrometer table. The angular velocity of the step motor can be controlled to enable tensile tests at different velocities. The interparticle distance is deduced from the displacement velocity and the duration of the step displacement. The velocity used for our tests was sufficiently low,  $5 \mu\text{m/s}$ , to avoid viscous effects.

Distilled water is introduced between two beads of 10 mm diameter via a channel in the upper bead connected to the water supply. The lower bead is attached to a high precision balance ( $10^{-3} \text{g}$ ) which monitors variations in mass during the tensile test. The output of the balance is connected to a

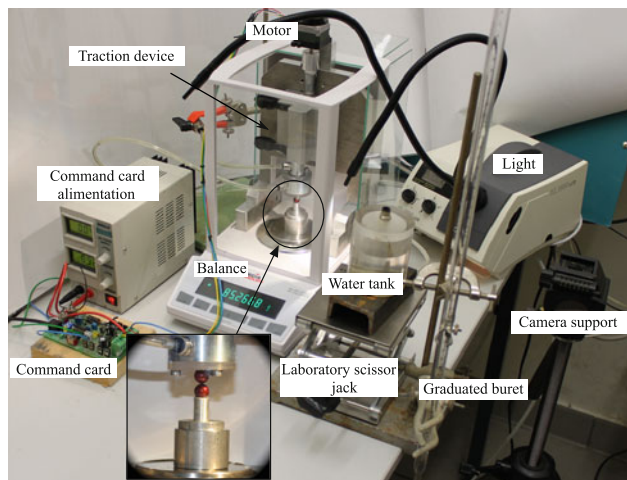


Fig. 1 Photo of the experimental device

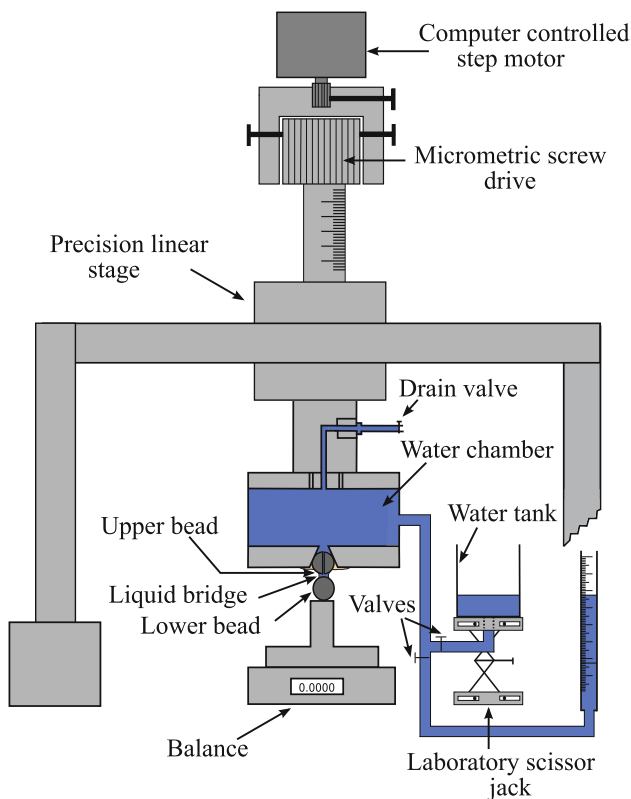


Fig. 2 Description of the experimental device

computer data logging system, which continuously records the apparent weight of the lower bead and its support as a function of time. The duration of the experiment is short (about 5 min).

The capillary force  $f_{cap}$  is calculated by differential weighting :

$$f_{cap} = (m_d - m_a)g \quad (1)$$

where  $m_d$  and  $m_a$  are respectively the dry mass and the apparent mass (in the presence of a liquid bridge) of the lower bead

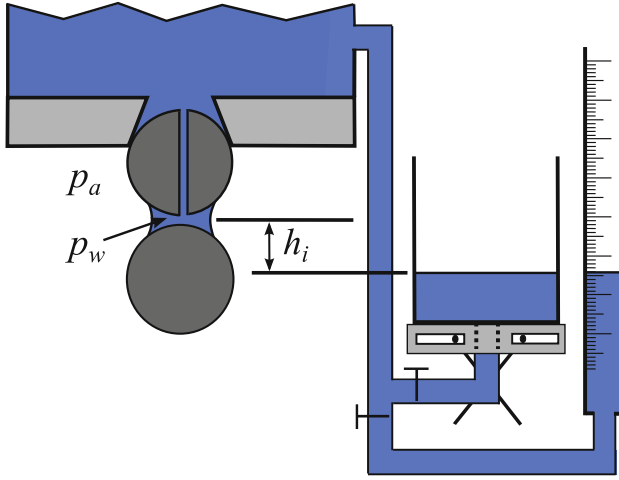


**Fig. 3** Details on the application of suction, which is deduced from the  $h_i$  measure

and its support. The bridge volume in our experiment was estimated to be in the  $0.1\mu l - 4\mu l$  range. It corresponds to a weight in the  $10^{-6} N - 0.4 \times 10^{-4} N$  range, which is relatively weak in comparison to the capillary force ( $10^{-4} N - 10^{-3} N$ ) but could be substantial in rare cases. Its effect contributes to decreasing the measured capillary force. The force that we measure would thus be an underestimation of the real capillary force. The liquid bridge volume and its weight was determined (using image analysis) and taken into account to compare the theoretical to the experimental results.

## 2.2 Suction control

The air pressure is the atmospheric pressure. The water pressure in the bridge is given by the difference  $h_i$  between the level of the liquid bridge neck and the level of the water in the water tank (Fig. 3). A hole in the upper bead ensures continuity between the liquid bridge water and the water of the water tank. The height of the water in the water tank is regulated by a laboratory scissor jack and measured by a graduated burette.

The Young-Laplace equation can be applied for the liquid bridge:

$$p_a - p_w = \gamma \left( \frac{1}{\rho_{ext}} - \frac{1}{\rho_{int}} \right) \quad (2)$$

where  $\rho_{ext}$  and  $\rho_{int}$  are respectively external and internal absolute values of radii of curvatures of the liquid bridge surface. At the level of the liquid bridge gorge, the internal radius of curvature is called the gorge radius  $h$ .

In the water tank and buret, water and air pressures are equal at the air-water interface. Suction  $s$  is thus defined by:

$$s = p_a - p_w = \rho g h_i \quad (3)$$

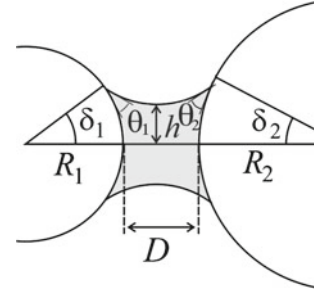


**Fig. 4** Geometrical model of a liquid bridge between two grains of different sizes:  $h$  is the gorge radius,  $D$  is the interparticle distance,  $\delta_1$  and  $\delta_2$  are the filling angles,  $\theta_1$  and  $\theta_2$  are the contact angles,  $R_1$  and  $R_2$  are the grain radii with  $R_1 \leq R_2$

Suction was not completely constant during the tensile test. As the upper bead rose,  $h_i$  changed during the test. Nevertheless, these changes could be easily evaluated and in most cases they were too weak in comparison to the initially imposed suction value because of the low rupture distance  $D_{rupt}$  of the liquid bridge.

In order to avoid air bubbles which may alter the water pressure control, a drain valve allowed the elimination of air bubbles (Fig. 2). A temperature of  $23^\circ C$  was kept throughout the experiments.

## 2.3 Image analysis

For given geometrical characteristics (grain radius, interparticle distance) of the grain-pair (Fig. 4), and given physical characteristics (contact angles, liquid/air surface tensions), we examined the effect of suction on the liquid bridge behaviour. The image analysis allowed us to measure the main liquid bridge characteristics.

A digital camera with macrozoom allowed us to accurately record the shape of the liquid bridge during the tensile test at the rate of one picture every 5 sec. It also allowed us to control the alignment of the two beads.

An image analysis program was developed to extract the main liquid bridge characteristics from the photos. Each bead boundary was fitted by a circle which enabled us to determine the scale of the photos (Fig. 5). First, the left and right profiles  $y(x)$  of the liquid bridge were detected and estimated by a fourth order polynomial. It was then possible to localize the contact point between the liquid bridge and the beads. Then the main geometrical characteristics of the liquid bridge were evaluated (Fig. 6):

- Gorge radius. We localized the minimum A and B of the right and left profiles (Fig. 5). The gorge radius is half of the distance between these minimums.
- Filling angles. These are determined according to the centers of the beads and the contact points.

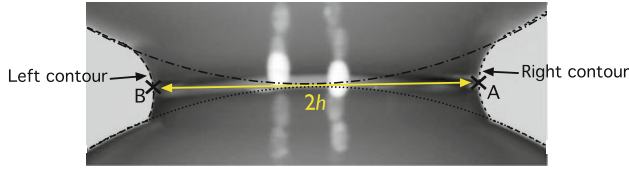


**Fig. 5** Detection of the beads and liquid bridge contours by image analysis

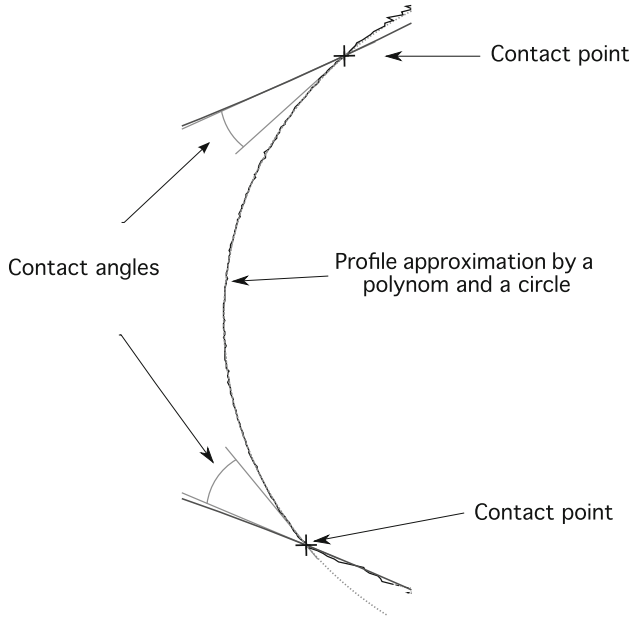


**Fig. 6** Details of the right contour by image analysis

- Contact angles. Contact angles are the angles between bead boundaries and polynomial representations of the liquid bridge (Fig. 6).
- Volume. The volume is obtained by calculating the surface covered by the liquid bridge while assuming that it is a surface of revolution (see Fig. 7):

$$V = \pi \int_{x_{c1}}^{x_{c2}} y^2(x) dx - V_1 - V_2 \quad (4)$$

#### 2.4 Experimental protocol

The first step involves filling the hydraulic system with water. For this, the hole of the upper bead is stopped up. Then water is added via the water tank until water flows off the drain valve. Then the drain valve is closed and the hole of the upper bead is opened. Water flows through the hole until  $h_i = 0$ . Then a liquid bridge is formed for  $h_i = 0$  by positioning the lower bead. By moving the water tank vertically and setting it at a given height, suction is applied to the liquid bridge. The tensile test can begin by applying a vertical velocity to the upper bead.

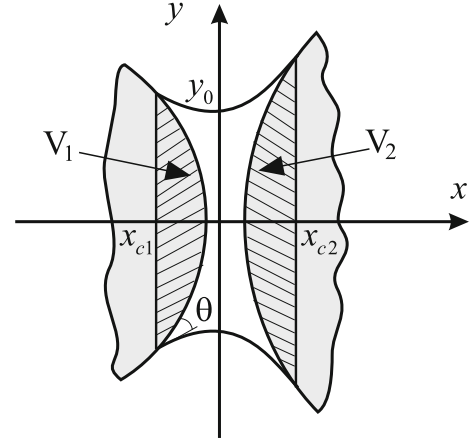


**Fig. 7** Details of the liquid bridge

### 3 Experimental results

The tensile tests were carried out with suction control. The granular material used for the experiments were monodisperse beads of 10 mm grain diameter. Figure 8 shows the variations in the liquid bridge during three steps of the tensile test. We noted that the liquid bridge formed was quite symmetrical during the test.

#### 3.1 Force and volume as a function of the interparticle distance at constant suction

Several tests were conducted for different suction values (Fig. 9). The results were highly repeatable (very low standard deviation). The behaviour was very close to the solutions of the Young-Laplace equation:

- In the case of tensile tests with suction control, the function representing the relation between the capillary force and the interparticle distance was monotonically decreasing and convex (Fig. 9) instead of concave as reported in tensile tests with volume control [13, 16, 18].
- The rupture distance decreased with increased suction (Fig. 9).
- For weak interparticle distances, the capillary force increased with increased suction (Fig. 9).
- For large interparticle distances, the capillary force decreased with increased suction (Fig. 9).

The influence of suction on variations in the capillary force as a function of the interparticle distance in tensile tests with suction control was found to be the opposite of the influence of volume in tensile tests with volume control. No peaks were noted in tensile tests with suction control, as generally observed in tensile tests with volume control [13, 18]. Such peaks have been previously attributed to changes in contact

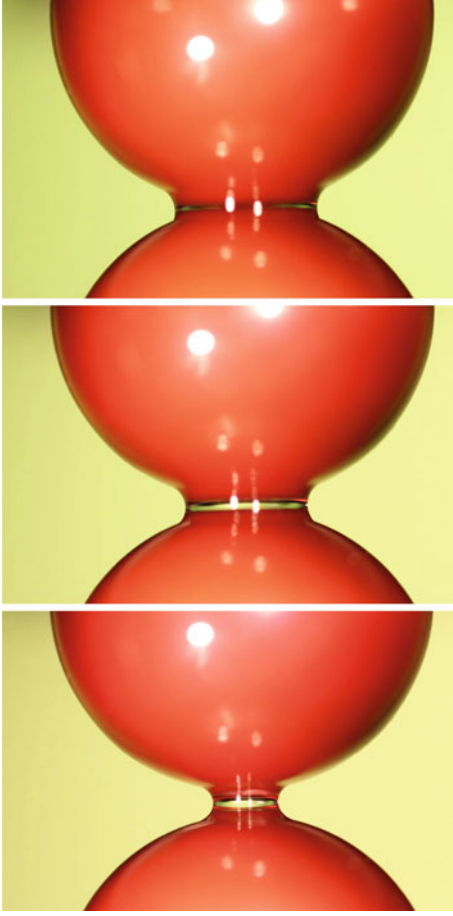


**Fig. 8** Photos of the liquid bridge. From the *top* to *bottom* photos, the interparticle distance is 0.0 mm, 0.3 mm and 0.67 mm (near rupture), respectively;  $R = 5$  mm and  $s \approx 40$  Pa

angles at low interparticle distance  $D$  values [18]. Moreover, we noted that variations in volume during the tensile test were not monotonic (Fig. 10). The volume first increased with the interparticle distance and finally decreased until rupture of the liquid bridge.

### 3.2 Experimental validation of the gorge method

The “gorge method” is conventionally used to calculate the capillary force. In this method, the capillary force  $f_{cap}$  is defined as a function of the gorge radius  $h$ , suction  $s$  and surface tension  $\gamma$ , and is expressed as:

$$f_{cap} = 2\pi\gamma h + \pi s h^2 \quad (5)$$

Surface tension is first measured at the outlet of the hydraulic system by wrenching ( $\gamma = 0.051$  N/m), suction is applied, and the gorge radius can be measured by image analysis. The low water surface tension value is attributed to impurities in the hydraulic system.

Figure 11 presents variations in the gorge radius as a function of the interparticle distance.

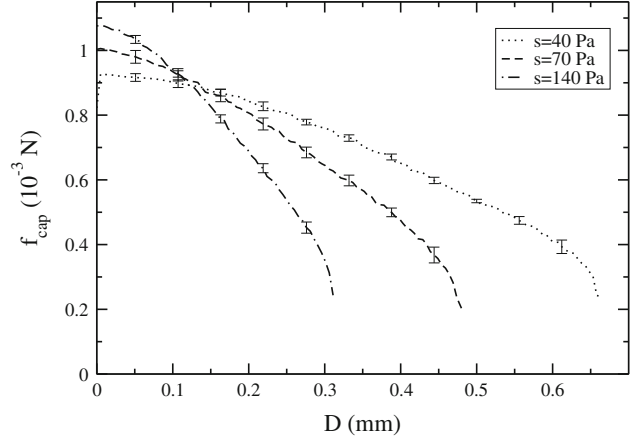


**Fig. 9** Variations in capillary force as a function of the interparticle distance in the case of tensile tests with suction control. Each point represents the average of 6 points

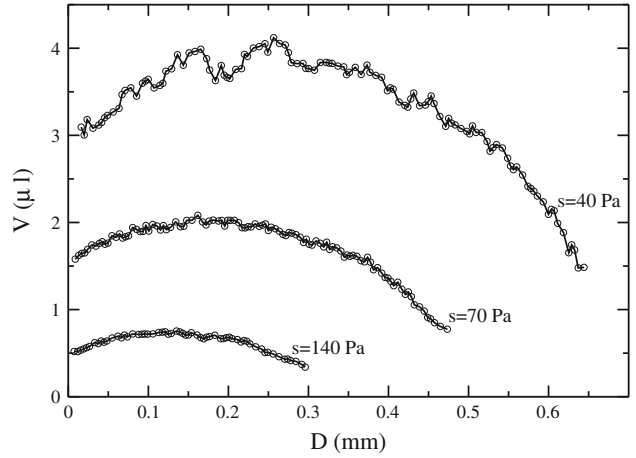


**Fig. 10** Experimental variations in liquid bridge volume as a function of the interparticle distance in the case of tensile tests with suction control

Experimental gorge radius, water surface tension and suction values were used to determine the capillary force using the “gorge method”. Capillary forces determined by the “gorge method” were very close to the experimental capillary forces (Fig. 12). For the comparison, we took into account the weight of the liquid bridge, which was calculated from its volume  $V$  measured by image analysis. The “gorge method” appears to be a good approximation to evaluate capillary forces for a symmetrical liquid bridge.

## 4 Force displacement and rupture modelling

Experimental capillary forces were compared to the solutions of the Young-Laplace equation. The “grain-pair” characteristics are known: grain radius ( $R = 5$  mm), surface tension ( $\gamma = 0.051$  N/m) and variations in the contact angle  $\theta$  with the interparticle distance  $D$  [19]. Some effects are due to gravity: upper top and lower bottom contact

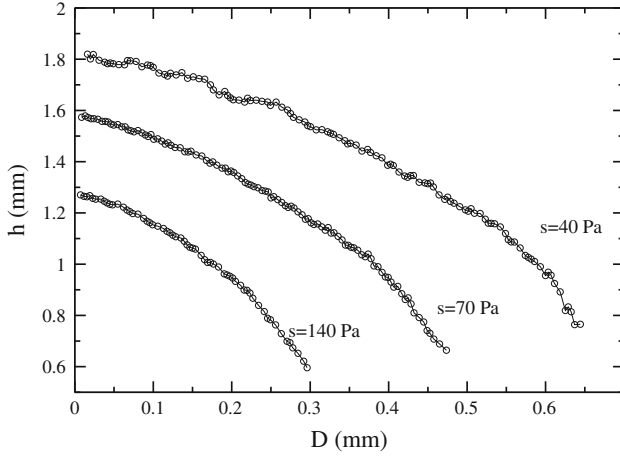


**Fig. 11** Experimental variations in the gorge radius measured by image analysis as a function of the interparticle distance and for different suction levels in the case of tensile tests with suction control

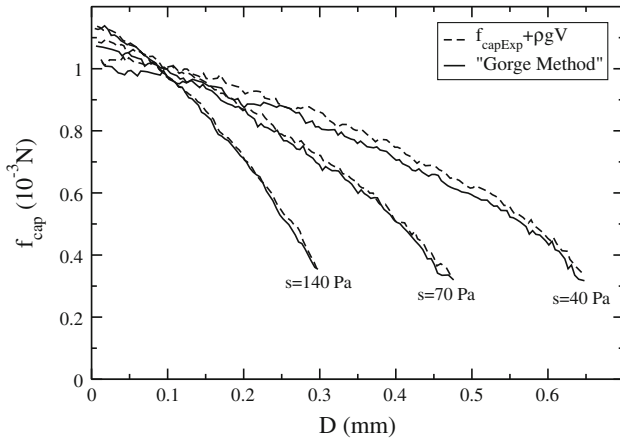


**Fig. 12** Comparison of experimental results obtained with the “gorge method” (Eq. 5) for different suction levels in the case of tensile tests with suction control

angles do not have the same value. We noted that the difference between both decreased with increased suction. In order to simulate the experimental behaviour, experimental variations in the upper and lower contact angles were fitted and then taken into account in the model. Then, by using the grain-pair characteristics during the tensile test, it was possible to compare the Young-Laplace solutions, associated with the “Gorge method”, to the experimental data in terms of capillary forces or rupture distances [20]. We noted that the experimental and theoretical capillary forces were very close (Fig. 13). The approximation was better for high suction levels. Otherwise, we noted that the gap between the theoretical approximation and the experimental data increased as a function of the interparticle distance. This increase could be explained by the gravity effect, which is greater for high interparticle distances (Appendix 1).

In tensile tests with controlled volume, an empirical expression proposed by Lian et al. [21], is generally used

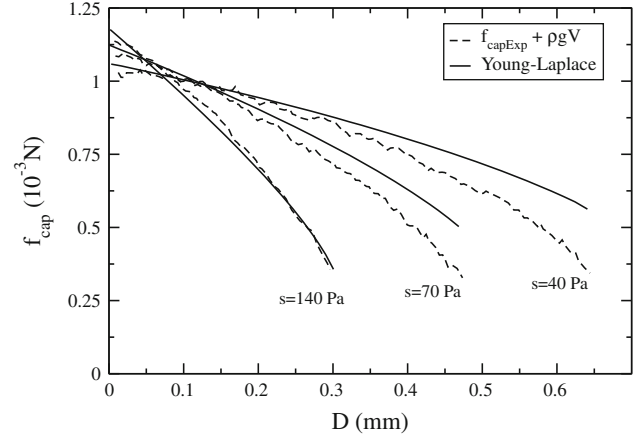


**Fig. 13** Comparison of the experimental results with Young-Laplace solutions concerning the capillary force for different suction levels in the case of tensile tests with suction control

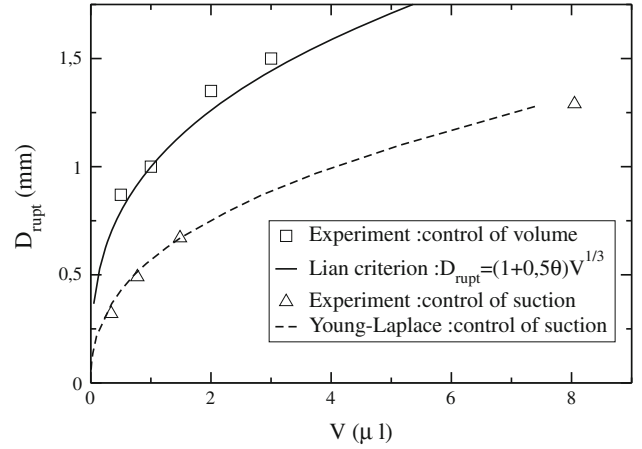


**Fig. 14** Rupture distance in tensile tests with controlled suction or volume ( $\theta = 20^\circ$ )

to predict the rupture distance of the liquid bridge. The Lian criterion of rupture is expressed as:

$$D_{rupt} = (1 + 0.5\theta) V^{\frac{1}{3}} \quad (6)$$

Firstly, the validity of this criterion in tensile tests with volume control was tested experimentally with our device. For this particular test, the upper bead did not have a hole and the volume was introduced between the two beads using a microsyringe. In this case, the Lian criterion gave a good prediction of the rupture distance as a function of the volume (Fig. 14): experimental data (square) are close to the Lian criterion. Secondly, the validity of this expression in tensile tests with suction control was tested experimentally. In this case, we noted as expected that the experimental data (triangles) were not in agreement with the Lian criterion but fit well the estimation of rupture from Young-Laplace equation (Fig. 14). These results clearly confirm that the rupture distance depends on the loading path of the liquid bridge.

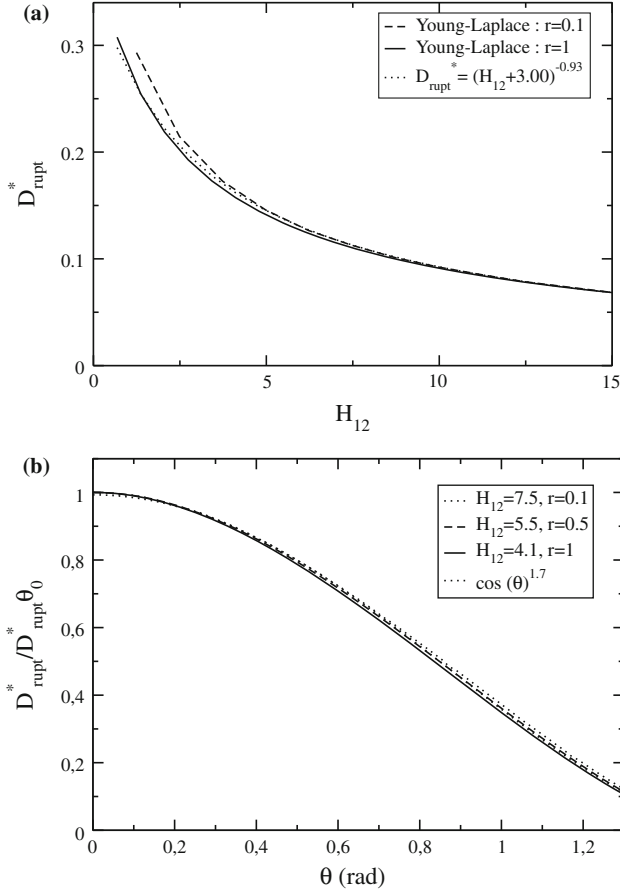


**Fig. 15** Tensile tests with suction control. **a** Variations in  $D_{rupt}^*$  as a function of  $H_{12}$  for  $\theta = 0$ . **b** Variations in the ratio  $\frac{D_{rupt}^*}{D_{rupt}^* \theta_0}$  for several  $r$  and  $H_{12}$  values as a function of the contact angle  $\theta$

A rupture criterion would be necessary for tensile tests with suction control. In this part, the results are presented with dimensionless variables. For grains with different radii  $R_1$  and  $R_2$ , we used the arithmetic mean radius  $R_{12} = \frac{2R_1 R_2}{R_1 + R_2}$ , the interparticle dimensionless distance  $D^* = \frac{D}{R_{12}}$  and the dimensionless suction  $H_{12} = \frac{\gamma R_{12}}{\gamma}$ . We noted that the relation between the dimensionless rupture distance and the dimensionless suction hardly depended on the polydispersity ratio  $r = \frac{R_1}{R_2}$  for  $0, 1 \leq r \leq 1$  in tensile tests with suction control (Fig. 15a) for null contact angles. We only plotted curves for  $r = 0.1$  and  $r = 1$ , but the other curves for  $0, 1 < r < 1$  are included in the space between the two plotted curves. From this observation, the dimensionless rupture distance for a null contact angle  $D_{rupt}^* \theta_0$  can be approximated by:

$$D_{rupt}^* \theta_0 = (H_{12} + 3)^{-0.93} \quad (7)$$

On Fig. 15b, we note that the relation between the ratio  $\frac{D_{rupt}^*}{D_{rupt}^* \theta_0}$  and the contact angle  $\theta$  hardly depends on the polydispersity ratio  $r$  for  $0.1 \leq r \leq 1$  and on the dimensionless suction  $H_{12}$  and follows a cosine curve. From this observation,

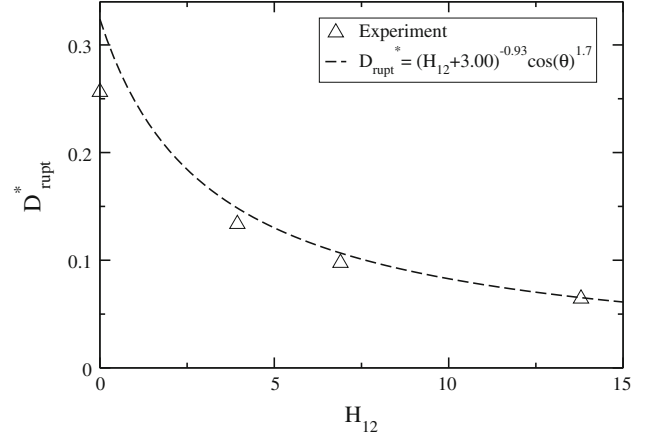


**Fig. 16** Rupture criterion for tensile tests with suction control ( $\theta = 20^\circ$ )

we formulated the following equation:

$$\frac{D_{rupt}^*}{D_{rupt}^* \theta_0} = (\cos \theta)^{1.7} \quad (8)$$

Finally, it is possible to establish a rupture criterion of the bridge which gives the dimensionless rupture of the liquid bridge as a function of the dimensionless suction  $H_{12}$  and contact angle  $\theta$  from Eqs. 7 and 8. Its expression is:

$$D_{rupt}^* = (H_{12} + 3)^{-0.93} * (\cos \theta)^{1.7} \quad (9)$$

This rupture criterion fit well the estimation of rupture from Young-Laplace equation. We noted that, for a mean contact angle of  $20^\circ$ , as measured by image analysis, the rupture criterion was very close to the experimental data for rupture (Fig. 16).

## 5 Conclusion

An innovative experimental device has been developed for tensile tests at constant suction and allows measurement of the main liquid bridge characteristics (capillary force, interparticle distance, liquid bridge volume, gorge radius, contact angles, filling angles) with excellent repeatability. This device also enables validation of an expression commonly used to calculate the capillary force, i.e. the ‘‘gorge method’’. A model based on the Young-Laplace equation coupled with the gorge method for calculation of the capillary force is proposed. This model specifically takes into account differences in contact angle between the liquid and two different grains. Our comparison between Young-Laplace solutions and experimental results concerning capillary forces indicated very close values. The validity of the Lian criterion for rupture did not seem to agree in the case of tensile tests with suction control. A criterion which depends on the dimensionless suction and contact angle is proposed for tensile tests with suction control. This result is very useful for studying



the effect of capillarity on the overall cohesion of a granular material because the density of liquid bridges is directly linked to the rupture distance of liquid bridges.

### Appendix: Effect of gravity

We consider a vertical liquid bridge under gravity. The effect of gravity decreases the rupture distance, creates distortion in the liquid bridge and changes the capillary forces. Under gravity, a difference of pressure  $\Delta p$  across the liquid/air interface is:  $\Delta p = \Delta p_0 - (\rho_w - \rho_a)gx$  [22,23].  $\rho_w$  et  $\rho_a$  are respectively densities of water and air,  $g$  is the acceleration due to gravity,  $\Delta p_0$  is the pressure difference between water and air at the liquid bridge gorge and  $x$  is the vertical position from the gorge section. Then, for a vertical liquid bridge with  $x$  defining the vertical axis, consideration of the gravity on the liquid bridge shape modifies the Young-Laplace differential equation, which becomes:

$$\frac{-\Delta p_0}{\gamma} + \frac{(\rho_w - \rho_a)g}{\gamma}x = \frac{\ddot{y}(x)}{(1 + \dot{y}^2(x))^{\frac{3}{2}}} - \frac{1}{y(x)\sqrt{1 + \dot{y}^2(x)}} \quad (10)$$

From this equation, we note that the effect of gravity increases with the interparticle distance [24]. The dimensionless equation becomes:

$$H = H_{12}^0 + B_0x^* = \frac{\ddot{y}^*(x^*)}{(1 + \dot{y}^{*2}(x^*))^{\frac{3}{2}}} - \frac{1}{y^*(x^*)\sqrt{1 + \dot{y}^{*2}(x^*)}} \quad (11)$$

with  $y^*(x) = \frac{y(x)}{R_{12}}$ ,  $x^* = \frac{x}{R_{12}}$ ,  $H_{12}^0 = \frac{-\Delta p_0 R_{12}}{\gamma}$  and  $B_0 = \frac{(\rho_w - \rho_a)g R_{12}^2}{\gamma}$ . In the experimental studies presented, the maximum ratio between the two left terms of the former equation was noted when  $x$  was high. Hence, the variation in water pressure inside the bridge increases as the interparticle distance increases. For example, in the above experiments, the maximum value of this ratio (at rupture) was respectively under 2, 7 and 15 % for suctions of 140 Pa, 70 Pa and 40 Pa. This means that the variation in water pressure inside the bridge due to gravity increases when suction decreases. This explains why the model was more accurate at high suction values. Considering that errors due to gravity are not very marked, we do not have to take gravity into account in our model. Nevertheless, its effects are of interest when analyzing the results.

### References

1. Schiffer, P.: Granular physics: a bridge to sandpile stability. *Nat. Phys.* **1**, 21–22 (2005)
2. Richefeu, V., El Youssoufi, M.S., Azéma, E., Radjai, F.: Force transmission in dry and wet granular media. *Powder Technol.* **190**, 258–263 (2009)

3. Scheel, M., Seemann, R., Brinkmann, M., Di Michiel, M., Shepard, A., Herminghaus, S.: Liquid distribution and cohesion in wet granular assemblies beyond the capillary bridge regime. *J. Phys.: Condens. Matter* **20**, 494236, (7pp.) (2008)
4. Mikami, T., Kamiya, H., Horio, M.: Numerical simulation of cohesive powder behavior in a fluidized bed. *Chem. Eng. Sci.* **53**(10), 1927–1940 (1998)
5. Pitois, O., Moucheron, P., Chateau, X.: Liquid bridge between two moving spheres: an experimental study of viscosity effects. *J. Colloid Interface Sci.* **231**, 26–31 (2000)
6. Soulié, F., El Youssoufi, M.S., Cherblanc, F., Saix, C.: Capillary cohesion and mechanical strength of polydisperse granular materials. *Eur. Phys. J. E* **21**, 349–357 (2006)
7. Richefeu, V., El Youssoufi, M.S., Peyroux, R., Radjai, F.: A model of capillary cohesion for numerical simulations of 3d polydisperse granular media. *Int. J. Numer. Anal. Methods Geomech.* **32**(11), 1365–1383 (2008)
8. Molenkamp, F., Nazemi, A.H.: Interactions between two rough spheres, water bridge and water vapour. *Géotechnique* **53**, 255–264 (2003)
9. Likos, J.W., Lu, N.: Hysteresis of capillary stress in unsaturated granular soil. *J. Eng. Mech.* **130**, 646–655 (2004)
10. Lechman, J., Lu, N.: Capillary force and water retention between two uneven-sized particles. *J. Eng. Mech.* **134**(5), 374–384 (2008)
11. El Shamy, U., Gröger, T.: Micromechanical aspects of the shear strength of wet granular soils. *Int. J. Numer. Anal. Methods Geomech.* **32**, 1763–1790 (2008)
12. Scholtès, L.: Modélisation Micro-Mécanique des Milieux Granulaires Partiellement Saturés. PhD thesis, Institut National Polytechnique de Grenoble, (2008)
13. Mason, G., Clark, W.C.: Liquid bridges between spheres. *Chem. Eng. Sci.* **20**, 859–866 (1965)
14. Hotta, K., Takeda, K., Linoya, K.: The capillary binding force of a liquid bridge. *Powder Technol.* **10**, 231–242 (1974)
15. Soulié, F.: Cohésion par capillarité et comportement mécanique de milieux granulaires. PhD thesis, Université Montpellier 2, (2005)
16. Willet, C.D., Adams, M.J., Johnson, S.A., Seville, J.P.K.: Capillary bridges between two spherical bodies. *Langmuir* **16**, 9396–9405 (2000)
17. Willet, C.D., Adams, J.M., Johnson, S.A., Seville, J.P.K.: Effects of wetting hysteresis on pendular liquid bridges between rigid spheres. *Powder Technol.* **130**, 63–69 (2003)
18. Soulié, F., Cherblanc, F., El Youssoufi, M.S., Saix, C.: Influence of liquid bridges on the mechanical behaviour of polydisperse granular materials. *Int. J. Numer. Anal. Methods Geomech.* **30**, 213–228 (2006)
19. Gras, J.-P.: Approche micromécanique de la capillarité dans les milieux granulaires: rétention d'eau et comportement mécanique. PhD thesis, Université Montpellier 2 (2011)
20. Gras, J.-P., Delenne, J.-Y., Soulié, F., El Youssoufi, M.S.: DEM and experimental analysis of the water retention curve in polydisperse granular media. *Powder Technol.* **208**, 296–300 (2011)
21. Lian, G., Thornton, C., Adams, J.M.: A theoretical study of the liquid bridge forces between two rigid spherical bodies. *J. Colloid Interface Sci.* **161**, 138–147 (1993)
22. Rotemberg, Y., Boruvka, L., Neumann, A.W.: Determination of surface tension and contact angle from the shapes of axisymmetric fluid interfaces. *J. Colloid Interface Sci.* **93**(1), 169–183 (1983)
23. Zeinali, Heris S., Hamed Mosavian, M.T.: Capillary holdup between vertical spheres. *Brazilian J. Chem. Eng.* **26**, 695–704 (2009)
24. Mazzone, D.N., Tardos, G.I., Pfeffer, R.: The effect of gravity on the shape and strength of a liquid bridge between two spheres. *J. Colloid Interface Sci.* **113**, 544–556 (1986)